

## Instruments and Methods

# In situ measurements of firn compaction profiles using borehole optical stratigraphy

Robert L. HAWLEY,\* Edwin D. WADDINGTON

*Department of Earth and Space Sciences, University of Washington, Seattle, Washington 98195-1310, USA  
E-mail: Robert.L.Hawley@Dartmouth.Edu*

**ABSTRACT.** We have developed a technique in which we use a borehole video camera and post-processing software to make a record of the optical brightness as a function of depth in polar firn. We call this method borehole optical stratigraphy. To measure firn compaction, we note the positions of optical features on the borehole wall detected by an initial ‘baseline’ log. We track the displacements of these features in subsequent logs. The result provides a measurement of the relative vertical motion and thus compaction of the firn over the survey period. We have successfully used this system at Summit, Greenland, to measure the depth distribution of firn column shortening experienced in a borehole over three 1 year periods. The uppermost 30 m of the firn at Summit is compacting as predicted by a simple steady-state model, implying that the firn density profile at Summit is at or close to steady state over the past ~70 years.

### INTRODUCTION

Detailed borehole measurements of vertical motion in ice and snow have been made in the past using several techniques (Paterson and others, 1977; Raymond and others, 1994; Hamilton and Whillans, 1996; Hawley and others, 2002; Elsberg and others, 2004). In polar firn, measurements of vertical motion can add valuable information to a glaciological field program. For example, such measurements can provide insight into the mechanics of firn compaction by constraining the actual rates of compaction (Arthern and others, 2010), and they can be used to assign a depth–age relationship to the shallow sections of an ice core (Hawley and others, 2002).

Altimetry measurements from aircraft or spacecraft can determine the surface height of an ice sheet, and mass balance can be estimated from changes in this height (Helsen and others, 2008). However, this height change involves several factors, including isostatic rebound, accumulation variability, ice flow, and firn compaction. In situ measurements of densification can help in the estimation of mass balance by radar or laser altimetry, by determining the amount of motion of the surface that is due to firn compaction. This compaction could also have a seasonal cycle (Zwally and Li, 2002).

Traditionally, detailed profiles of vertical motion in boreholes required the placement of artificial markers in the firn. It was sometimes time-consuming and difficult to place these markers, and occasionally they were displaced by the measuring tool (Hawley and others, 2004). With the development of borehole optical stratigraphy (BOS; Hawley and others, 2003), we have overcome this limitation, and produced a technique that is detailed, accurate, fast, and easy to implement in the field. BOS emerged from a novel technique (Hawley and others, 2002) for determining the locations of metal marking bands, in an effort to measure a

profile of vertical strain. This technique compared favorably with the previous method, which used a metal-detecting tuned coil to locate the marking bands (Hawley and others, 2004). Subsequent studies revealed that BOS could distinguish annual layers in the firn (Hawley and others, 2003), and that the optical signal from BOS had a complex relationship with density (Hawley and Morris, 2006). BOS tracks the natural variations in density and grain size in the firn; these properties together produce the optical variations recorded by the borehole camera, making it possible to measure firn column shortening by tracking optical features.

### BOREHOLE OPTICAL STRATIGRAPHY

#### Overview

BOS is a borehole logging method that uses a video camera and image processing to measure the relative brightness of the wall of a borehole. In this way, we obtain information in situ that is similar to that which visual stratigraphers obtain from a core. Our vertical-motion measurement technique exploits the fact that the BOS log of a borehole contains distinctive features that can be identified and tracked as they move down in the firn column in subsequent logs.

#### Field methods

##### *Borehole preparation*

The borehole to be used for a BOS vertical-motion study can be a dry borehole to any depth. The hole should be drilled with an electromechanical drill, to keep the diameter variation to a minimum and maintain the physical structure of the firn (thermal drills would alter the grain structure). The hole must not be fully cased, because the camera must see the details of the firn in the borehole walls. A short casing is desirable, however, to minimize the damage to the top of the borehole from repeated transits of the camera. The casing should be clamped to a platform on the surface so that it does not affect compaction. A typical installation is sketched in Figure 1.

\*Present address: Department of Earth Sciences, Dartmouth College, Hanover, New Hampshire 03755, USA.

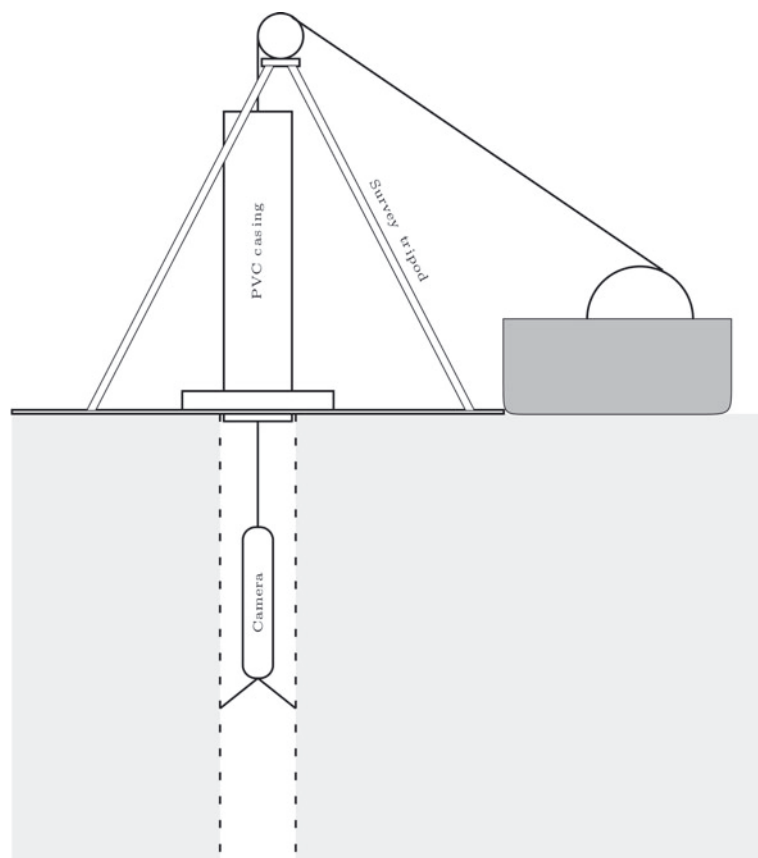


**Fig. 1.** Set-up of the system. An optical encoder on the sheave wheel measures the depth of the camera in the hole. The box on the snow surface contains the video-capture camera, winch, depth counter and electronics.

### Camera

The down-hole camera is a downward-looking, wide-angle Geovision Jr<sup>TM</sup> borehole camera. Using a charge-coupled device (CCD) sensor, the camera produces analog video. Illumination is provided by a set of white light-emitting diodes arranged in a circle around the CCD. The camera is supported in the hole by a three-conductor flat cable which carries both video signal and camera power. From the surface, the cable runs over a pulley and down to a motorized winch that raises and lowers the camera smoothly. The video signal exits the cable spool through slip-rings and then enters the video-overlay unit described below.

### Depth measurement

Depth is measured at the top of the borehole by an optical encoder from BEI Industrial Encoders, mounted to the shaft of the pulley. The encoder sends 1000 pulses per revolution on two channels as square waves with a 90° phase offset, a scheme known as quadrature encoding. A quadrature decoder can determine the direction of rotation of the pulley from the relative phase between the two channels. The circumference of the pulley is 0.32 m, resulting in a nominal depth resolution of 0.00032 m. The signal from the encoder is routed to the depth-counter/video-overlay unit. We calibrate the depth counter by attaching a surveyor's tape measure to the cable and lowering the instrument a short distance down the hole, measuring the distance with both devices. We repeat this procedure at several depths and thus with different amounts of weight on the pulley. In our experience, differing weights did not change the calibration, indicating that cable stretch is insignificant.

### Counter and overlay electronics

In order to co-register the depth measurement with each video frame, we overlay the depth on each frame. The depth-counter and video-overlay unit consists of a video-overlay circuit, a depth-counting circuit and a microcontroller. The depth-counting circuit receives the quadrature pulse signal from the encoder, decodes it and feeds it into a count register in the microcontroller. The microcontroller converts the depth to human-readable ASCII characters and sends it to the video-overlay circuit, which combines the text with the video signal, placing the depth on the upper left corner of the field of view. The combined signal is then routed for digitizing and storage to a digital video (DV) camcorder, which also serves as a field monitor for the down-hole camera. The entire unit is self-contained in a metal box of dimensions 0.65 m × 0.6 m × 0.52 m weighing 61 kg. The system runs on a.c. power, which is supplied by a 1 kW portable generator. Profiling speeds for this system are limited only by desired depth resolution. For example, at the DV frame rate of ~30 frames s<sup>-1</sup>, if we wish to sample a frame every 0.001 m, our logging speed is ~30 s m<sup>-1</sup>, and a complete log of one of our 30 m holes takes ~15 min.

### Data reduction

#### Video capture

We capture the raw DV signal to a computer using an IEEE 1394 interface and commercial video-editing software. Our in-house software reads the raw DV file and treats each frame individually. A typical frame is shown in Figure 2.

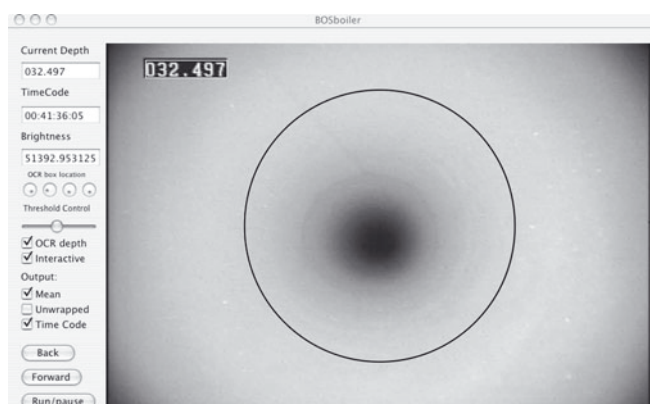


**Fig. 2.** A typical frame of the borehole video in our in-house software. The camera is looking straight down the borehole. Centralizers hold the camera close to the middle of the borehole. The black circle marks the annulus around the borehole wall. The in-house software calculates the average brightness of these pixels and reads the depth (upper left) for each frame using OCR. Note that the camera is not perfectly centered in the borehole. As described by Fudge and Smith (2010), this can cause subtle differences in the shapes of optical features, and may account for the uncertainty in our relative motion calculations.

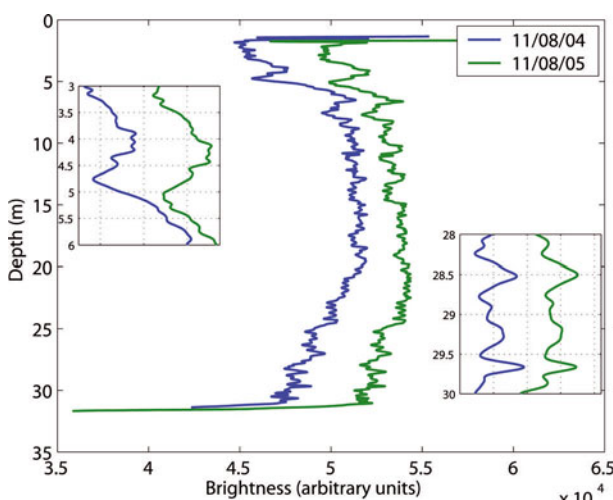


**Fig. 3.** One of the log pairs used in this case study. The raw logs have been co-registered at the bottom of the borehole and low-pass filtered. The arbitrary brightness value in each has been offset for display purposes; the total brightness change over the course of a year is minimal. Insets highlight the depth offset between common features in the shallow region, and the alignment of features at depth. We quantify these offsets to determine the relative vertical motion profile. Dates are mm/dd/yy.

### Image processing

For each frame, our in-house software reads the depth from the upper left corner of the frame using optical character recognition (OCR). The software then calculates the mean of the 16-bit brightness values in an annulus of pixels around the borehole wall (Fig. 2). The resulting depth-intensity series is the BOS profile. Figure 3 shows two such profiles, 1 year apart, from a shallow borehole at Summit, Greenland.

In practice, the OCR routine occasionally mistakes one character for another, resulting in depth errors. Usually these errors are easy to identify and correct because we can reasonably expect the depth series to be continuous with a relatively constant slope. An error in reading one digit will cause a discontinuity in the depth record where the OCR routine erred. The sections that contain erroneous depths can then be corrected manually.

### Test case: Greenland Summit

We used this system to measure relative vertical motion in an array of shallow boreholes at Summit camp, Greenland, at approximately 72.58° N, 38.47° W. The boreholes were drilled with the Ice Core Drilling Services ‘Prairie Dog’ electromechanical drill. These ~0.13 m diameter boreholes are ~30 m deep, covering the shallow region where firn compaction is most rapid. Science technicians stationed at the camp measured BOS profiles of the boreholes at monthly intervals. Here we present the result from several pairs of borehole logs taken in the same hole at ~1 year intervals.

## DETERMINING VERTICAL MOTION

### Co-registration of independent logs

Once we have two BOS logs taken at different times in the same borehole, we can determine the relative vertical motion that has taken place in the time between the two logs. Our technique relies on matching the same optical features identified in each of two logs. Because we are

interested in relative motion within the borehole, it is important to define a reference point where relative motion is zero. Our preferred reference point is at the bottom of the borehole, since it is intuitive to consider the layers above settling downward. Aligning the logs at the bottom is not a simple matter, however, as the features near the bottom of the hole have periodic shapes, resulting in multiple highly correlated matches. In practice, the choice of reference point is arbitrary, because our measured displacements are relative. For example, if the reference point is chosen at a middle depth of the log, features below that depth will ‘appear’ to be moving up, while features above will ‘appear’ to be moving down, but the shape of the relative displacement profile will be unchanged. Once the displacements have been measured, we can set the bottommost displacement to zero, and thus calculate all displacements relative to the bottom of the hole. Thus in theory, no co-registration is required. For computational ease, however, it is desirable for the two logs to line up to a zero displacement at some point along the profile (allowing a smaller ‘search area’; see below).

To align the two logs, we calculate cross-correlation of the full 30 m log with respect to depth, exploiting the fact that although the smaller features (which we later use for matching) are displaced, the 30 m scale curvatures of the logs are similar. This cross-correlation aligns the two logs correctly at one point in depth, which will result in an offset of zero in the subsequent processing to determine motion. Once we have a profile of relative motion, we subtract the mean apparent motion of the bottommost ten features to reference the entire profile relative to the bottom of the borehole.

Fudge and Smith (2010) used ray tracing to determine that the photons reaching the camera from the borehole wall have actually been scattered from many points along the borehole wall, not just from the point within the annulus (though this point would be the last point from which the photon scattered before entering the sensor). Fudge and Smith

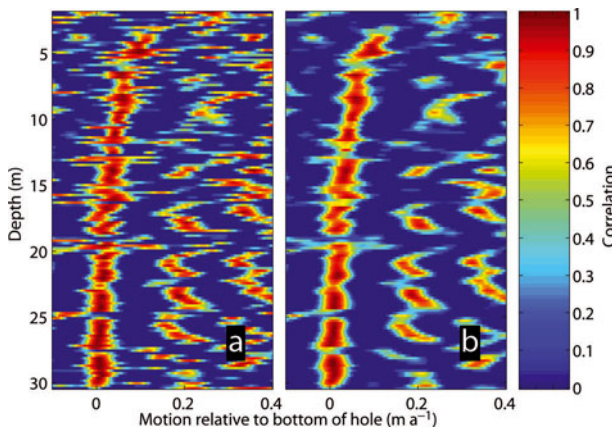


**Fig. 4.** Correlations as a function of depth and offset. For each depth/offset pair, the color indicates correlation. The matching correlations can be seen in the trail of red colors leading upward from offset of 0 at depth 30 m. The other high-correlation areas are due to spurious correlations within the BOS profile; offset the logs enough, and a given peak on the reference section will begin to spuriously correlate with a neighboring peak in the search area. (a) The raw correlations. (b) The correlations after treatment with a  $3 \times 3$  low-pass spatial filter.

(2010) showed that a feature could affect the brightness log as far as 10 cm away. Thus BOS itself acts as a low-pass filter on the actual stratigraphy. In our brightness log, to highlight the features of interest and to reduce noise, we process the raw log with a fourth-order Butterworth low-pass filter with a cut-off at 0.075 m. This value was chosen to be consistent with the findings of Fudge and Smith (2010), and verified experimentally based on repeatability tests that determined the shortest length-scale at which optical features were seen to be repeatable in two logs; non-repeatable features are interpreted as noise and are filtered out.

### Feature matching

As seen in Figure 3, common features can be identified by eye, and the offset between them can be measured as a function of their average depths. Thus a profile with depth of displacement relative to the bottom of the hole can be generated. For a more objective process, we turn to an automatic feature-matching routine, similar to the approach described by Scambos and others (1992) for two-dimensional (2-D) image correlation. For each pair of logs, we begin by defining a set of 160 overlapping ‘reference’ sections on the second log. Each reference section is in turn cross-correlated within a larger ‘search area’ on the first log.

The optical features that we use in the BOS log are most likely the annual depth-hoar/wind-slab couplet (e.g. Hawley and others, 2003). At Summit, based on a mean accumulation of  $0.25 \text{ m a}^{-1}$  (Meese and others, 1994), annual layers would be between 0.65 m at the surface and 0.25 m at the bottom of the firn. These lengths represent the likely natural length scale for features in our logs. Thus any given section of a log at least 0.5 m long should contain at least one peak or trough.

We choose the length scale of the reference section based on the length scale of the characteristic features we see. A reference section that is too short will be essentially featureless; it will be a line that will correlate with any other line of similar slope. A reference section that is too long will itself have been altered by the relative vertical

motion we wish to measure: features that have moved closer together will prevent a good correlation. Based on our characteristic feature size, we use a reference section of 0.5 m. Similarly, a search area that is too small might not contain the feature to be matched, and a search area that is too large may lead to spurious correlations with adjacent features. Where features match and offsets are correct, the correlation is high. Figure 4a shows the initial output of this process, correlations as a function of depth and offset. For each depth/offset pair, the color indicates correlation; though some outliers are evident, the true motion profile stands out. The high-correlation patches to the right in Figure 4a occur because subsequent features in a BOS profile are similar; offsetting one profile so that common features match results in high correlation, but increasing the offset by the distance between adjacent features results in a similarly high correlation with the subsequent feature.

To find the points where the correct features are matched up at high correlation, we use a  $3 \times 3$  2-D equally weighted moving-average (boxcar) smoothing filter on the matrix of correlations, resulting in a spatial filtering at length scales of 0.6 m on the depth scale and 0.005 m on the displacement scale. This filtering process tends to reduce this effect, while leaving the true correlations largely unchanged. The result of the filtering process is shown in Figure 4b.

To determine the set of points that make up a relative vertical motion profile, we begin by accepting only points with correlations greater than 0.9. Since some of the spurious high-correlation points also show correlations above this threshold, we additionally require that points accepted lie within a specified displacement from the zero reference (in this case, we chose 0.3 m as the maximum realistic displacement. At Summit an annual snow accumulation of approximately  $0.65\text{--}0.75 \text{ m}$  at an initial density of  $\sim 350 \text{ kg m}^{-3}$  will compress by  $\sim 0.3 \text{ m}$  to reach a density of  $600 \text{ kg m}^{-3}$  at 30 m (Hawley and Morris, 2006)). The final estimated relative vertical motion profiles for three 1 year periods are shown in Figure 5.

### Estimating uncertainty

As can be seen in Figure 2, the camera is not always perfectly centered in the borehole. Furthermore, though the camera will tend to follow the same path, this centralization or lack thereof is not uniquely repeatable from one log to the next. As shown by Fudge and Smith (2010), an off-center camera can have a significant impact on the recorded brightness of a particular feature, so even the shape of a feature might be subtly different from one log to the next, confounding the feature-matching scheme described above. Furthermore, though we take steps to ensure the camera cable does not slip as it passes over the pulley, we cannot exclude this possibility, which will impart a further error. To investigate the uncertainty associated with our estimates of relative motion, we tested the repeatability of the technique. We recorded 16 logs in four boreholes in a 50 m square on 21–22 May 2005. We recorded a single log in each of the same four boreholes on 31 May 2006. This yields 16 profiles of relative motion for the same time period. For each borehole we calculated a mean vertical motion profile, and calculated the standard deviation from that mean profile. The standard deviation did not show any significant trend with depth, indicating that uncertainty is random rather than systematic. The mean of all the standard deviation profiles was  $0.0106 \text{ m a}^{-1}$ . We take this value as our estimated

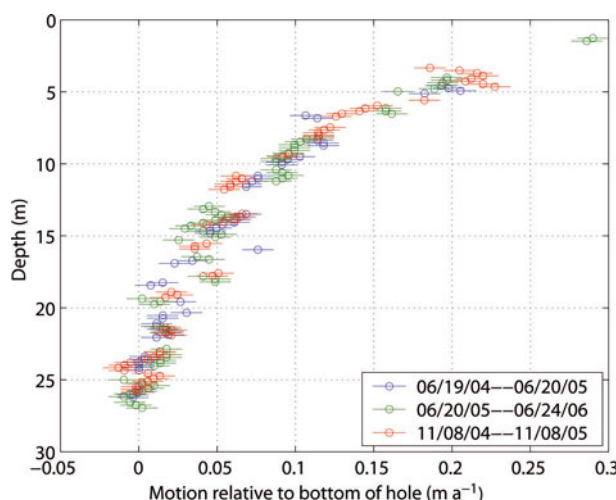


**Fig. 5.** Profiles of relative vertical motion in the ‘Phillips’ borehole at Summit, during three separate (but overlapping) 1 year intervals. Each point is plotted with a horizontal bar indicating the  $\sim 1 \text{ cm a}^{-1}$  confidence interval. Dates are mm/dd/yy.

uncertainty on any given depth-displacement point, and each point in Figure 5 is plotted with error bars of this dimension on each side.

## DISCUSSION

Here we compare our measured compaction profile with a modeled steady-state compaction profile, calculated from a measured density profile. Horizontal strain rates in the Summit area are  $\sim 4 \times 10^{-4} \text{ a}^{-1}$  (Hvidberg and others, 1997). The total accumulated dynamic strain due to ice flow on 70 year old firn near the bottom of our hole will be  $2.8 \times 10^{-3}$ . By comparison, firn at this depth has increased in density from  $350 \text{ kg m}^{-3}$  to  $600 \text{ kg m}^{-3}$ , experiencing a strain due to compaction of 0.4 (Hawley and others, 2008). Neglecting horizontal divergence, and assuming steady-state compaction (Sorge’s law; Paterson, 1994), the amount of water that falls as snow on the surface of the ice sheet must pass through an imaginary plane at depth corresponding to the bottom of the borehole, following mass continuity. Specifically, if  $\dot{b}$  is the average accumulation rate in ice equivalent units and  $\rho_{\text{bot}}$  is the density at the bottom of the borehole, the bottom of our borehole moves down in the ice sheet (primarily due to continued firn compaction) at a rate of  $\dot{b} \frac{\rho_{\text{ice}}}{\rho_{\text{bot}}}$ . Similarly, an imaginary material plane at any other depth,  $z$ , of our borehole moves down in the ice sheet at  $\dot{b} \frac{\rho_{\text{ice}}}{\rho(z)}$ , with  $\rho(z)$  the density at depth  $z$ . The difference between these two rates is the rate of shortening of the firn column,  $\Delta v(z, z_{\text{bot}})$ , between depth  $z$  and the bottom of the hole,  $z_{\text{bot}}$ . Thus, the profile of vertical velocity relative to the borehole bottom is

$$\Delta v(z, z_{\text{bot}}) = \dot{b} \left( \frac{\rho_{\text{ice}}}{\rho_{\text{bot}}} - \frac{\rho_{\text{ice}}}{\rho(z)} \right). \quad (1)$$

Hawley and others (2008) measured a high-resolution density profile in another borehole in our array,  $\sim 50 \text{ m}$  from the borehole used in this study. The accumulation rate,  $\dot{b}$ , is  $\sim 0.25 \text{ m a}^{-1}$  (Meese and others, 1994). Using the measured density profile, we use Equation (1) to calculate a predicted vertical velocity profile, with the assumptions of steady state and no horizontal divergence. Figure 6 shows the predicted

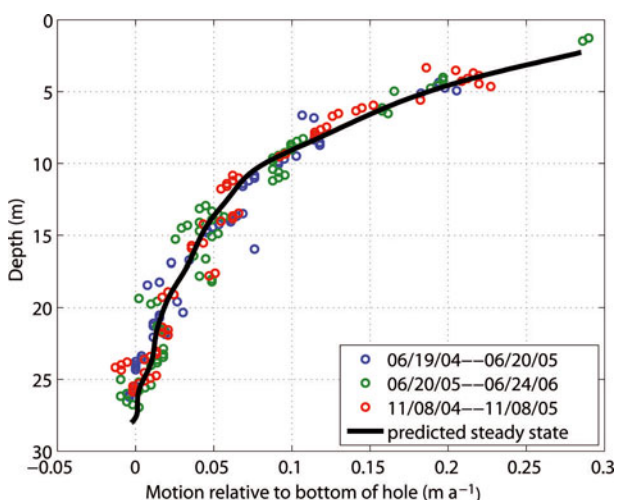


**Fig. 6.** Inferred vertical motion relative to the bottom of the hole from Figure 5, with a predicted profile of annual motion calculated from a density profile (Hawley and others, 2008), assuming steady-state accumulation of  $0.25 \text{ cm a}^{-1}$  (Meese and others, 1994) and no horizontal divergence. We low-pass filtered the  $1 \text{ cm}$  resolution density profile at  $1.5 \text{ m}$  scale to remove short-scale (interannual to seasonal) variations in density, and removed the filter end-effects. Dates are mm/dd/yy.

profile, along with the measured profiles from Figure 5. From the agreement between the measured profiles and that predicted by a simple steady-state model, we conclude that the firn density profile in the Summit area has been at or close to steady state over the period sampled by this borehole ( $\sim 70$  years; Hawley and others, 2008).

As a further check on our measurements, we use Equation (1) with measured values of density near the bottom and top of our profile, and at the bottom of the firn (where  $\rho(z) \equiv \rho_{\text{ice}}$ ), and we calculate the expected  $\Delta v(z, z_{\text{bot}})$ , where  $z_{\text{bot}}$  is the bottom of the firn. Near the bottom of our borehole (25 m) where  $\rho(z) = 600 \text{ kg m}^{-3}$ , we find  $\Delta v(z, z_{\text{bot}}) = -0.13 \text{ m a}^{-1}$ . Near the top of our borehole (2.5 m) where  $\rho(z) = 350 \text{ kg m}^{-3}$ , we find  $\Delta v(z, z_{\text{bot}}) = -0.41 \text{ m a}^{-1}$ . The difference between the two values is  $-0.28 \text{ m a}^{-1}$ , in agreement with our topmost measurements of motion relative to the bottom of the hole (Fig. 5).

## CONCLUSIONS AND FUTURE WORK

In this study, we have demonstrated a method for measuring compaction in polar firn by BOS, using the natural optical features of the firn as markers. This method is fast (profiling a  $30 \text{ m}$  hole in  $15 \text{ min}$ ) and easy to implement in the field, and with simple analysis can provide a measure of the vertical motion in the firn as a result of firn compaction. The annual firn compaction at Summit agrees with the expected values from a simple steady-state model, implying that for the past  $\sim 70$  years the firn density profile at Summit has been at or close to steady state.

Because it can yield a profile of compaction from a single borehole, BOS can make detailed compaction measurements in polar firn. To characterize the change in surface elevation from firn densification for incorporation into altimetry studies (e.g. Arthern and Wingham, 1998), it is desirable to understand not only the vertical profile of firn compaction, but also its temporal and spatial variability.

Thus it is desirable to measure multiple sites affected by the same climate, to determine the short-scale spatial variability of firn compaction. Firn compaction has been found to be affected by fluctuations in temperature (Li and Zwally, 2002; Arthern and others, 2010), so the temporal variability of firn compaction should also be measured. By drilling only 30 m in this study, we recovered three-quarters of the firn compaction signal. Thirty metres is also below the depth to which seasonal temperature fluctuations will penetrate, so temporal variability in densification could be investigated by making more frequent logs. Because the instrumentation is inexpensive, relatively easy to use and permits fast data collection, BOS is well suited for these types of studies where it is desirable to characterize many sites at high temporal and spatial resolution.

## ACKNOWLEDGEMENTS

We thank Veco Polar Resources for field support. The boreholes used for this study were drilled by Ice Core Drilling Services. We are grateful to the Summit science technicians for field measurements, troubleshooting and assistance. We thank L. Kehrl for assistance with data processing. This paper benefited greatly from insightful reviews by D. Breton, A. Svennson and the scientific editor, D. Peel, and we thank them. This work was completed in part with the support of the Center for Advanced Research Technology in the Arts and Humanities (CARTAH) at the University of Washington, and was financially supported by the US National Science Foundation under grants OPP-0087521 and OPP-0352584. This work is dedicated in memory of Gregg Lamorey, friend and colleague.

## REFERENCES

- Arthern, R.J. and D.J. Wingham. 1998. The natural fluctuations of firn densification and their effect on the geodetic determination of ice sheet mass balance. *Climatic Change*, **40**(4), 605–624.
- Arthern, R.J., D.G. Vaughan, A.M. Rankin, R. Mulvaney and E.R. Thomas. 2010. In situ measurements of Antarctic snow compaction compared with predictions of models. *J. Geophys. Res.*, **115**(F3), F03011. (10.1029/2009JF001306.)
- Elsberg, D.H. and 6 others. 2004. Depth- and time-dependent vertical strain rates at Siple Dome, Antarctica. *J. Glaciol.*, **50**(171), 511–521.
- Fudge, T.J. and B.E. Smith. 2010. Light propagation in firn: application to borehole video. *J. Glaciol.*, **56**(198), 614–624.
- Hamilton, G.S. and I.M. Whillans. 1996. Global positioning system measurements of ice-sheet mass balance using the ‘coffee-can’ method. *Antarct. J. US*, **31**(2), 86–88.
- Hawley, R.L. and E.M. Morris. 2006. Borehole optical stratigraphy and neutron-scattering density measurements at Summit, Greenland. *J. Glaciol.*, **52**(179), 491–496.
- Hawley, R.L., E.D. Waddington, D.L. Morse, N.W. Dunbar and G.A. Zielinski. 2002. Dating firn cores by vertical strain measurements. *J. Glaciol.*, **48**(162), 401–406.
- Hawley, R.L., E.D. Waddington, R.A. Alley and K.C. Taylor. 2003. Annual layers in polar firn detected by borehole optical stratigraphy. *Geophys. Res. Lett.*, **30**(15), 1788. (10.1029/2003GL017675.)
- Hawley, R.L., E.D. Waddington, G.W. Lamorey and K.C. Taylor. 2004. Vertical-strain measurements in firn at Siple Dome, Antarctica. *J. Glaciol.*, **50**(170), 447–452.
- Hawley, R.L., E.M. Morris and J.R. McConnell. 2008. Rapid techniques for determining annual accumulation applied at Summit, Greenland. *J. Glaciol.*, **54**(188), 839–845.
- Helsen, M.M. and 7 others. 2008. Elevation changes in Antarctica mainly determined by accumulation variability. *Science*, **320**(5883), 1626–1629.
- Hvidberg, C.S., D. Dahl-Jensen and E.D. Waddington. 1997. Ice flow between the GRIP and GISP2 boreholes in central Greenland. *J. Geophys. Res.*, **102**(C12), 26,851–26,859.
- Li, J. and H.J. Zwally. 2002. Modeled seasonal variations of firn density induced by steady-state surface air-temperature cycle. *Ann. Glaciol.*, **34**, 299–302.
- Meese, D.A. and 8 others. 1994. The accumulation record from the GISP2 core as an indicator of climate change throughout the Holocene. *Science*, **266**(5191), 1680–1682.
- Paterson, W.S.B. 1994. *The physics of glaciers. Third edition.* Oxford, etc., Elsevier.
- Paterson, W.S.B. and 7 others. 1977. An oxygen-isotope climatic record from the Devon Island ice cap, Arctic Canada. *Nature*, **266**(5602), 508–511.
- Raymond, C.F., J.C. Rogers, P.L. Taylor and B. Koci. 1994. Vertical strain measurement in core holes. *Mem. Natl Inst. Polar Res.*, Special Issue 49, 234–240.
- Scambos, T.A., M.J. Dutkiewicz, J.C. Wilson and R.A. Bindschadler. 1992. Application of image cross-correlation to the measurement of glacier velocity using satellite image data. *Remote Sens. Environ.*, **42**(3), 177–186.
- Zwally, H.J. and J. Li. 2002. Seasonal and interannual variations of firn densification and ice-sheet surface elevation at Greenland summit. *J. Glaciol.*, **48**(161), 199–207.

MS received 20 August 2010 and accepted in revised form 27 November 2010